PCCP

Accepted Manuscript

ROYAL SOCIETY OF CHEMISTRY

www.rsc.org/pccp

Journal Name

RSCPublishing

ARTICLE

Imaging fenestrations in liver sinusoidal endothelial cells by optical localization microscopy

Cite this: DOI: 10.1039/xoxxooooox

Viola Mönkemöller[a], Mark Schüttpelz[a], Peter McCourt[b], Karen Sørensen[b], Bård Smedsrød[b], and Thomas Huser[a,c]

Received ooth January 2012,
Accepted ooth January 2012

DOI: 10.1039/xoxxooooox

www.rsc.org/

Liver sinusoidal endothelial cells (LSEC) are an important class of endothelial cells facilitating the translocation of lipoproteins and small molecules between the liver and blood. A number of clinical conditions, especially metabolic and aging-related disorders, are implicated by improper function of LSECs. Despite their importance, research into these cells is limited because the primary ultrastructures involved in their function are transcellular pores, called fenestrations, with diameters in a size range between 50-200 nm, i.e. well below the optical diffraction limit. Here, we show that we are able to resolve fenestrations with a spatial resolution of ~20 nm by *direct* stochastic optical reconstruction microscopy (*d*STORM). The cellular plasma membrane was labeled at high fluorophore density with CellMask Deep Red and imaged using a reducing buffer system. We compare the higher degree of structural detail that *d*STORM provides to results obtained by 3D structured illumination microscopy (3D-SIM). Our results open up a path to image these physiologically important cells in vitro using highly resolving localization microscopy techniques that could be implemented on non-specialized fluorescence microscopes, enabling their investigation in most biomedical laboratories without the need for electron microscopy.

Introduction

During the last decade, a number of very powerful techniques have been established to overcome the diffraction limit in the optical far-field resulting in a spatial resolution at the nanoscale[1-8]. Up to now, the vast majority of these techniques relied on fluorescent probes and use techniques to modify their fluorescent properties to achieve optical super resolution[1]. This has enabled an increasing number of very exciting applications in biology and biomedical research, but also in materials science and chemistry. In the majority of cases, however, only structures that can be fluorescently labeled have been studied[9]. A number of very relevant and interesting biological structures, on the other hand, cannot be fluorescently labeled, because no specific probes have yet been identified or exist. Examples for such structures are pores in the plasma membrane of endothelial cells that often serve important physiological functions. Liver sinusoidal endothelial cells (LSECs), in particular, contain a large number of these unique morphological features[10]. LSECs separate blood from the extracellular space of Disse and surrounding sheets of hepatocytes. LSECs are essential for life and their impaired function with increasing age has been implicated in the onset of many aging-related diseases. Also, their loss (e.g. due to paracetamol poisoning) leads to acute liver failure and death[11]. LSECs are responsible for the efficient clearance of macromolecules and small particles, such as metabolites, pharmaceutical drugs, oxidized lipoproteins, and small viruses from the blood[12, 13]. In addition they have a very important ultrafiltration function, allowing direct passage of lipoproteins between hepatocytes and blood.

To support their filter function, LSECs contain a large number of non-diaphragmed pores, called fenestrations, with diameters ranging between 50 and 200 nm. Fenestrations are arranged into groups, called sieve plates that can spread over 20% of the LSEC's surface. The size of fenestrations is, however, well below the optical resolution limit and there are no specific cell surface markers for fenestrations. Therefore, their observation has, until recently, been limited to electron microscopy, which might introduce fixation artifacts, and cannot be used for living cells.

Previously, we were able to image these structures using three-dimensional structured illumination microscopy (3D-SIM)[14, 15]. While enabling the visualization of fenestrations, 3D-SIM is, in the linear case, limited to a spatial resolution of approximately 100 nm in the best case, leaving questions about its ultimate applicability to the study of processes that affect the size and shape of fenestrations unanswered. Here, we demonstrate the use of single molecule localization microscopy (*direct* stochastic optical reconstruction microscopy, *d*STORM[8, 16-19]) for resolving structural details of fenestrations in LSECs. To enable this we have optimized the photochemical behavior of CellMask Deep Red Plasma Membrane Stain, which has not yet been used for *d*STORM, and compared our new results to results obtained with 3D-SIM. This opens the door for a range of new studies that could utilize the complementarity of super resolution techniques, where e.g. one method is utilized to rapidly scan for relevant features, while another method is then used subsequently to enable the observation of structural details with highest spatial resolution.

Materials and Methods

Materials Reagents included Type 1A Collagenase (Sigma Chemical, St. Louis, MO #C9891), RPMI (Gibco Invitrogen #11875-093), and CellMask Deep Red Plasma Membrane Stain (Life Technologies, #C10046).

Cell Culture Sprague Dawley male rats (Scanbur BK, Sollentuna, Sweden) were kept under standard conditions and fed standard chow ad libitum (Scanbur, Nittedal, Norway). The experimental protocols were approved by the Norwegian National Animal Research Authority (NARA) in accordance with the Norwegian Animal Experimental and Scientific Purposes Act of 1986. The rats (body wt 150–300 g) were anesthetized with a mixture of medetomidin (Domitor vet, Orion, Turku, Finland) and ketamine (Ketalar, Pfizer, New York, NY) and LSECs were isolated and purified as described [20] and plated on fibronectin coated #1.5 coverslips for 3h in RPMI-1640. The LSECs were then fixed with 4% paraformaldehyde (PFA) in phosphate buffered saline (PBS) and 0.02M sucrose, pH 7.2 for 15 min, and stored under PBS.. Following fixation the cells were prepared for visualization using *d*STORM.

Fluorescent Staining of LSECs The fixed samples were washed with PBS to remove unwanted residuals. The LSECs were stained with CellMask Deep Red plasma membrane stain at a concentration of 5 µg/ml for 10 min at room temperature. The staining solution was removed and the samples were carefully washed with PBS 2-3 times. For better background reduction the use of Tween 20 at 0.01% concentration proved to be beneficial.
For dye post-fixation 3.7% PFA was applied for 10 min at room temperature. Then the PFA was removed and the sample was again washed 2-3 times with PBS. Imaging was conducted in PBS buffer (adjusted to pH 7.4) with an oxygen scavenger system (glucose oxidase, catalase, glucose) and 100 mM ß-mercaptoethylamine [16].

Super resolution imaging of LSECs For super resolution imaging we used single molecule localization microscopy of conventional fluorophores (*d*STORM). We used an Olympus IX71 microscope equipped with an oil immersion objective (PlanApo 60x NA 1.45, Olympus) in the objective-type TIRF/HILO configuration to reduce the amount of out of focus light.
To enable controlled blinking of individual fluorophores, the CellMask stain was simultaneously illuminated by two continuous wave laser beams of an ArKr-ion laser (Innova 70C, Coherent) which were selected by an acousto-optic tunable filter (AOTF). The 647 nm line was used for excitation while the 488 nm line was used for activation of the fluorophores. A dichroic filter (FF502/670) was used to separate the excitation/activation light from the emitted fluorescence signal. Fluorescence images were acquired at high frame rates by an EMCCD camera (DV887DCS-BV, Andor) with emission filters (Bandpass 700/75, Longpass 647LP, Chroma Filters) directly mounted to the camera in order to remove residual laser excitation light. For each measurement the laser power was adjusted in such a way that single fluorophores appear as dense as possible while being well separated for single molecule localization. In addition, the blinking rate had to be adjusted to the acquisition rate resulting in laser power densities of approximately 1-2 kW/cm² at the sample.
Typically, for the final reconstruction of a super-resolved image up to 40,000 frames were acquired and analyzed by the open source reconstruction software *rapid*STORM[21, 22]. Due to acquisition times of several minutes and a localization accuracy of a few tens of nanometers, sample drift has a significant negative effect on sharpness and contrast of the reconstructed images. Therefore, images were initially corrected for sample drift by assuming a linear drift using the built-in drift correction of *rapid*STORM. To maximize the benefits of drift correction, we also developed an automated drift assessment tool. To further improve the visibility of fenestrations, all *d*STORM images in this paper are treated with a 2 pixel-wide (~14 nm) Gaussian blur filter in the open-source software *Fiji*.

3D-SIM images of LSECs were acquired following the same staining protocols using a commercial structured illumination microscope (DeltaVision|OMXv4.0 BLAZE, GE Healthcare).

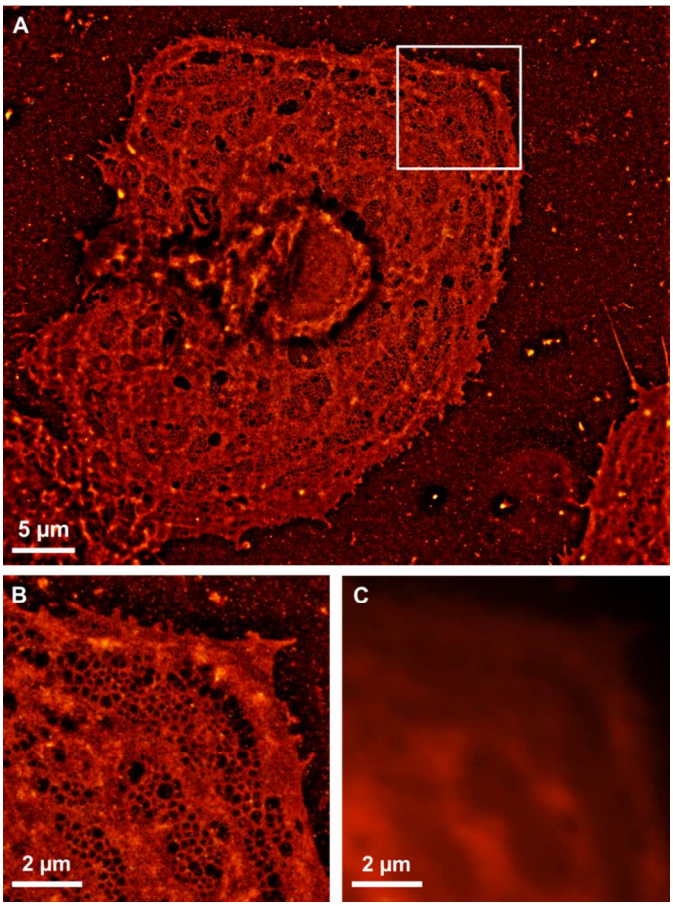

Fig.1. (A) *d*STORM image of a liver sinusoidal endothelial cell (LSEC) plated on a fibronectin-coated glass coverslip, stained with 5 µg/ml CellMask Deep Red, and post-fixed with 3.7% PFA. The single frame exposure time was 29.55 ms, and a total of 13,483 frames were used in this reconstruction, resulting in a total acquisition time of ~7 min. The region highlighted in **(A)** is shown magnified in **(B)** and compared to the conventional widefield microscopy image **(C)**. Sieve plates and individual fenestrae can be seen as dark spots against the bright background from the plasma membrane.

Results

To visualize the LSEC plasma membrane, we utilized CellMask Deep Red Plasma Membrane Stain, a lipophilic fluorophore which is an excellent live and fixed cell membrane stain for cellular plasma membranes. CellMask stains have been used in our previous studies based on 3D structured illumination microscopy[14, 15]. To the best of our knowledge, CellMask Deep Red has not yet been used for single molecule localization microscopy, e.g. *d*STORM, and its chemical structure is proprietary to the manufacturer. We initially tried a

number of alternative fluorophores (DiI, DiO, Fluorophore-wheat germ agglutinin) none of which worked well in our hands, so that eventually we worked out an appropriate protocol that resulted in excellent stochastic blinking behavior of CellMask. Thus, we conducted all the experiments reported in this contribution using CellMask Deep Red for *d*STORM.

Figure 1A shows the reconstructed *d*STORM image of an entire LSEC based on localizing individual fluorophores of the membrane stain in 13,483 frames. Characteristic cellular structures can readily be identified based on this image. The nucleus in the center is clearly distinguishable from the circumference of the cell. Delicate, thin structures, such as filopodia reaching out of the neighboring cell on the right hand side of the figure are observed distinctly. Most notably, this cell contains a large number of sieve plates with dimensions of up to several few microns (see Figure 1B for a magnified view of the area outlined in Fig. 1A). Each sieve plate contains tens of fenestrae with a mean diameter on the order of ~ 100 nm. The outer cell region is well suited for *d*STORM imaging due to thinness of the plasma membrane, which worked well for the TIRF/HILO configuration used for exciting fluorescence. In the vicinity of the nucleus fewer details are observed for two reasons. First, much of the nucleus is outside of the focal plane due to its larger dimension in z direction. Second, due to the presence of multiple membranes surrounding the nucleus as well as the endoplasmic reticulum, the CellMask stain is significantly agglomerated near the nucleus resulting in a local stain concentration that is too high to resolve with single molecule based localization methods. For comparison, Figure 1C shows the magnified ROI acquired in the conventional fluorescence mode in the same TIRF/HILO configuration equivalent to the super-resolved image in Figure 1B. The image is almost featureless and only dark regions embedded in brighter surroundings are visible providing hints of the location of sieve plates. Only through correlation with the accompanying *d*STORM image can these regions clearly be identified as sieve plates. In the super-resolved image the fenestrations appear as well-defined holes in the membrane with dimensions below the optical diffraction limit.

To evaluate our results we compared them to another state-of-the-art super resolution microscopy technique. Figures 2A and 2B show a 3D-SIM image and a magnified view of a similar (but different) LSEC, also stained with CellMask Deep Red using the same protocols as for *d*STORM imaging. For comparison, another set of *d*STORM images are shown in Figures 2C and 2D. Both methods are clearly capable of resolving the fenestrations, however it is quite apparent that *d*STORM is able to reveal even smaller fenestrations that cannot be resolved by 3D-SIM. In addition, *d*STORM is able to resolve very thin membranes that sometimes divide individual fenestrae that are seen as one single feature in 3D-SIM (see Figs. 3 and 4 for such examples). Also, both super-resolution microscopy techniques permit a quantitative analysis of the pore diameter of the fenestrations by utilizing a pore area analysis tool (Volocity, PerkinElmer).

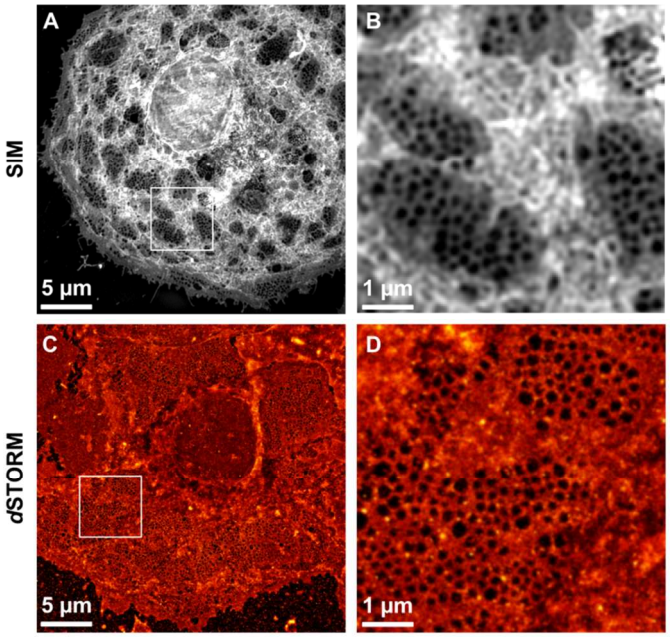

Fig.2. **(A)** Structured illumination microscopy image of a representative single LSEC stained with CellMask Deep Red. **(C)** *d*STORM image of a similar cell where the intrinsically higher resolution of localization microscopy becomes apparent. Single frame exposure time: 20.40 ms, 40,000 frames, total recording time: ~14.5 min. **(B)** and **(D)** are magnifications of the regions highlighted in **(A)** and **(C)**, showing several sieve plates.

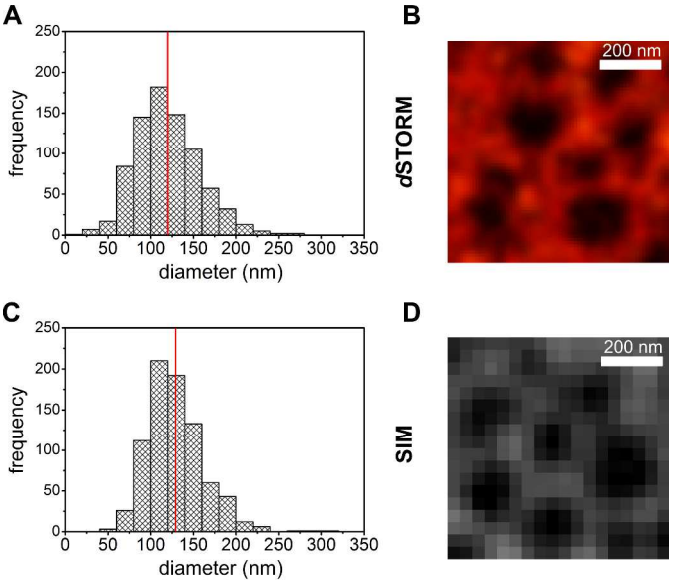

Fig.3. **(A)** Histograms of the fenestration diameters imaged by *d*STORM (evaluated from Figure 2C) and 3D-SIM (evaluated from Figure 2A) measured by determining the full-width half minimum of 800 fenestrae, each. Both histograms show a normal distribution with a mean diameter of 129.1 nm (SIM) and 119.8 nm (*d*STORM) (red lines). **(B)** Enlargement of a 720 x 720 nm² area to show differences in details of *d*STORM and SIM reconstructions. *d*STORM (upper right) performs localization with ~20 nm accuracy, resulting in the resolution of fine details such as dividing membranes.

Since *d*STORM can in principle achieve a localization precision of about 20 nm it enables the observation of smaller structures than

what can be resolved by SIM, which is limited to about 100 nm. Interestingly, the mean pore diameter observed by *d*STORM is 119.8 ± 37.6 nm, which is very similar to that obtained by SIM with 129.1 ± 33.1 nm. *d*STORM measurements do, however, result in a much broader distribution of pore diameters, which is clearly related to the improved spatial resolution with which a wide range of fenestrations can be measured. In a few cases, fenestrae with a diameter of less than 50 nm can be counted.

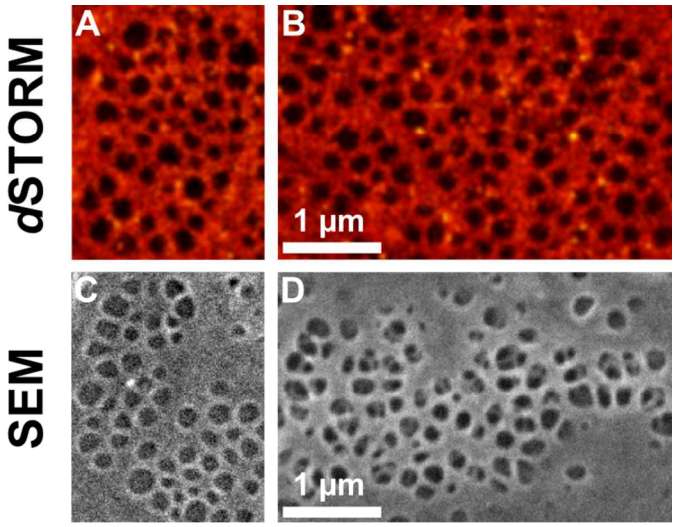

Fig.4. Comparison of LSEC fenestrae and sieve plates imaged by **(A, B)** *d*STORM and **(C, D)** scanning electron microscopy (SEM). This direct comparison demonstrates nicely how *d*STORM achieves a resolution similar to that obtained by SEM, but in wet, fixed LSEC preparations. Remarkably, the non-circular substructure seen by SEM is now also resolved optically.

Discussion

Utilizing the cell membrane stain CellMask Deep Red combined with a specifically adapted staining protocol, we were able to resolve submicroscopic morphological structures with a negative contrast, so-called cellular fenestrations, by single molecule localization microscopy. The reproduction of an inverse structure such as pores in a membrane is a challenge for single molecule based microscopy techniques such as *d*STORM and PALM. So far, *d*STORM was typically used to image distinct cellular structures whose constituents can be stained, such as the cytoskeleton, mitochondria, vesicles, or nuclear pore complexes. In contrast, to enable the successful reconstruction of a surface containing holes, the surface has to be stained with a dense and homogeneous distribution of a fluorophore that can undergo rapid photoswitching. The lack of specific markers for fenestrations and the high fluorophore density make it difficult to ensure that no secondary, unlabeled regions that might appear as artificial (i.e. not existing) holes in the surface are imaged. Also, overlaps between single blinking events need to be avoided. To image very tiny structures, background fluorescence caused by unspecific binding of fluorophores to the substrate (e.g. glass coverslips) has to be minimized. The requirements for appropriate staining protocols are therefore more difficult to fulfill than those when positive structures are labeled. In our case, after experimenting with a range of fluorophores, we found that only the lipophilic dye CellMask resulted in reliable staining of LSEC membranes that enabled the visualization of fenestrae over a wide range of diameters. This, combined with TIRF/HILO excitation of the fluorophores, allowed us to observe fenestrations with diameters as small as 50 nm.

Remarkably, when viewed at the level of individual sieve plates, the rather nonsymmetric substructure of fenestrae, which typically appeared as round holes when imaged by 3D-SIM, can be seen. This is demonstrated in Figure 4, where *d*STORM images of sieve plates are compared to similar data (again, from different cells) obtained by scanning electron microscopy (SEM). In a number of cases (see e.g. the upper half of Fig. 4A), we also observe thin membranes crossing fenestrae, reminiscent of similar structures seen in Fig. 4D, that indicate the three-dimensional nature of these structures crossing the cell's cytoplasm. This indicates that in the future, *d*STORM and other optical super-resolution microscopies can be used to replace the more elaborate and expensive procedures required to view fenestrations by SEM. Furthermore, multiple structures can be stained and imaged in optical microscopy simultaneously, and it has the potential to ultimately enable imaging of fenestration dynamics in living LSECs. While extending 3D-SIM to living cells is rather straight-forward and has been demonstrated multiple times, since only 9-15 SIM frames have to be acquired in order to reconstruct a single plane[23-25], live cell imaging by *d*STORM is more cumbersome because even in the best of cases thousands of frames have to be acquired in order to reconstruct useful images from *d*STORM data[22, 26]. Visualization of image structures with negative contrast, such as fenestrations, will likely require the acquisition of even more individual frames. To explore the minimum number of frames required to still resolve fenestrae, we took one of our data sets and consistently reduced the total number of frames that were used for image reconstruction. Key to successfully achieving the lowest possible number of frames was, again, the fact that we employed an automated drift correction routine for the image sequence. Figure 5 shows a sequence of images, where the number of frames used to reconstruct the image has been consistently lowered from 10,000 to 2,000. As can be seen from this figure, some fenestrae can still be identified even if just 2,000 frames were used for the reconstruction. By employing faster EMCCD cameras or sCMOS cameras, approximately 1,000 frames can be acquired in 1s, which indicates, that even *d*STORM imaging of fenestration dynamics could be achieved on the order of 1-2 seconds for each final, reconstructed image.

Conclusions / Outlook

We have demonstrated *d*STORM imaging of morphological features in the cellular plasma membrane that provide negative contrast, i.e. which cannot be stained directly. Pore diameters of individual fenestrae with a diameter of less than 50 nm were identified. We also found that typical fenestrae have an appearance that does not necessarily resemble round holes, similar to what was observed in SEM images. As few as 2,000 frames were deemed necessary to successfully reconstruct sieve plates in the plasma membrane of LSECs by *d*STORM. This could potentially be reduced to even fewer frames by employing others means of analyzing and reconstructing the data, e.g. based on sliding window averaging, or by conducting a fluctuation analysis[27], e.g. by super-resolution optical fluctuation imaging (SOFI)[28], which will ultimately enable imaging of the fenestration dynamics in living cells. The fluorophore used in our work is perfectly capable of staining the membrane of living cells and based on preliminary SIM imaging also appears to have no detrimental effect on the number or structure of fenestrae when compared to fixed cells.

Based on these results, it is apparent that it should now be possible to image LSEC fenestration morphology based on a technique that can be used to equip even standard fluorescence microscopes with super-resolution capabilities at a very low cost, making it accessible to a much larger range of biomedical research laboratories[29].

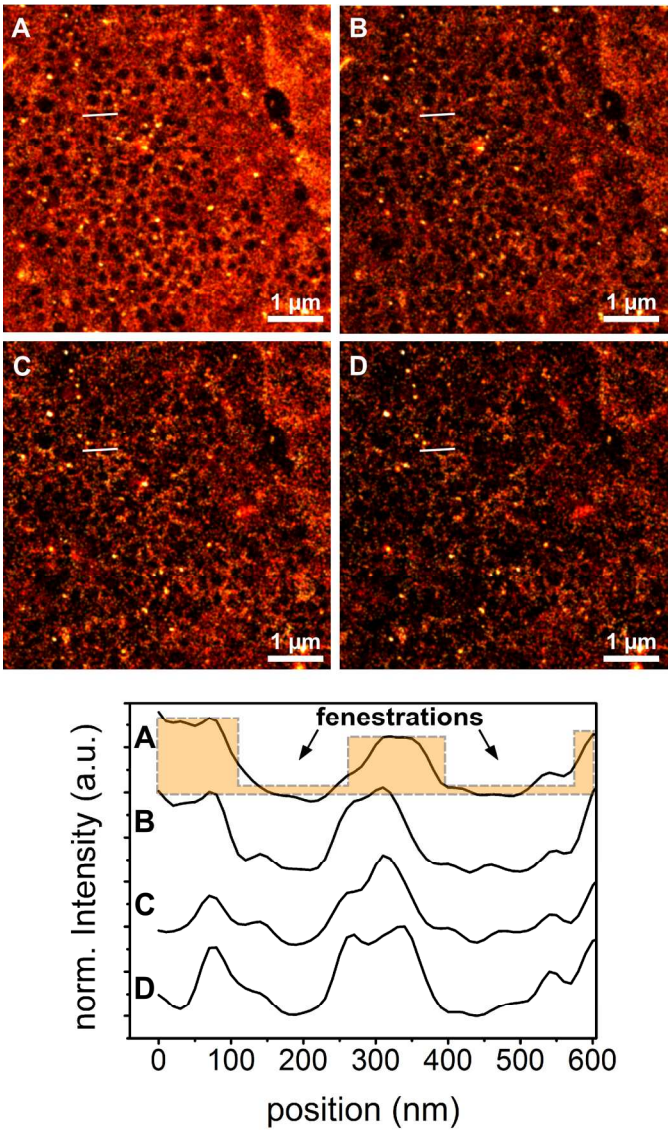

Fig.5. Continuous reduction of the number of frames used to reconstruct a sieve plate. The number of frames are **(A)** 10,000, **(B)** 5,000, **(C)** 3000, and **(D)** 2,000. Cross-sections of the same location in each image are shown below the image sequence. This indicates that some fenestrae can still be identified if as few as 2,000 frames have been acquired, potentially enabling rapid live cell imaging of fenestration dynamics.

Acknowledgements

This work was supported in parts by the Ministry of Innovation, Science, Research and Technology of the State of North Rhine-Westphalia (MIWFT) as part of the research cooperation "MoRitS - Model-based Realization of intelligent Systems in Nano- and Biotechnologies" (grant no. 321 - 8.03.04.03 - 2012/02), and the Tromsø Research Foundation (supported by Trond Mohn).

Notes and references

[a] Biomolecular Photonics, Department of Physics, University of Bielefeld, 33615 Bielefeld, Germany.
[b] Medical Biology, University of Tromsø, Tromsø, Norway.
[c] Dep. of Internal Medicine, University of California, Davis, Sacramento, CA 95817, USA.

1. S. W. Hell, *Science*, 2007, **316**, 1153-1158.
2. S. W. Hell and J. Wichmann, *Opt Lett*, 1994, **19**, 780-782.
3. E. Betzig, G. H. Patterson, R. Sougrat, O. W. Lindwasser, S. Olenych, J. S. Bonifacino, M. W. Davidson, J. Lippincott-Schwartz and H. F. Hess, *Science*, 2006, **313**, 1642-1645.
4. E. Betzig, *Opt Lett*, 1995, **20**, 237-239.
5. M. J. Rust, M. Bates and X. W. Zhuang, *Nat Methods*, 2006, **3**, 793-795.
6. M. G. L. Gustafsson, L. Shao, P. M. Carlton, C. J. R. Wang, I. N. Golubovskaya, W. Z. Cande, D. A. Agard and J. W. Sedat, *Biophys J*, 2008, **94**, 4957-4970.
7. M. G. L. Gustafsson, D. A. Agard and J. W. Sedat, *P Soc Photo-Opt Ins*, 2000, **1**, 141-150.
8. M. Heilemann, S. van de Linde, M. Schuttpelz, R. Kasper, B. Seefeldt, A. Mukherjee, P. Tinnefeld and M. Sauer, *Angew Chem Int Ed Engl*, 2008, **47**, 6172-6176.
9. T. Huser, *Curr Opin Chem Biol*, 2008, **12**, 497-504.
10. F. Braet and E. Wisse, *Comp. Hepatol.*, 2002, **1**.
11. Y. Ito, N. W. Bethea, E. R. Abril and R. S. McCuskey, *Microcirculation*, 2003, **10**, 391-400.
12. K. K. Sørensen, P. McCourt, T. Berg, C. Crossley, D. Le Couteur, K. Wake and B. Smedsrød, *Am J Physiol Regul Integr Comp Physiol*, 2012, **303**, R1217-1230.
13. L. P. Ganesan, S. Mohanty, J. Kim, K. R. Clark, J. M. Robinson and C. L. Anderson, *Plos Pathog*, 2011, **7**, e1002281.
14. D. Svistounov, A. Warren, G. P. McNerney, D. M. Owen, D. Zencak, S. N. Zykova, H. Crane, T. Huser, R. J. Quinn, B. Smedsrod, D. G. Le Couteur and V. C. Cogger, *Plos One*, 2012, **7**.
15. V. C. Cogger, G. P. McNerney, T. Nyunt, L. D. DeLeve, P. McCourt, B. Smedsrod, D. G. Le Couteur and T. R. Huser, *J Struct Biol*, 2010, **171**, 382-388.
16. S. van de Linde, A. Loschberger, T. Klein, M. Heidbreder, S. Wolter, M. Heilemann and M. Sauer, *Nat Protoc*, 2011, **6**, 991-1009.
17. S. van de Linde, U. Endesfelder, A. Mukherjee, M. Schuttpelz, G. Wiebusch, S. Wolter, M. Heilemann and M. Sauer, *Photoch Photobio Sci*, 2009, **8**, 465-469.
18. M. Heilemann, S. van de Linde, A. Mukherjee and M. Sauer, *Angew Chem Int Ed Engl*, 2009, **48**, 6903-6908.
19. S. van de Linde, M. Sauer and M. Heilemann, *J Struct Biol*, 2008, **164**, 250-254.
20. B. Smedsrod, H. Pertoft, G. Eggertsen and C. Sundstrom, *Cell Tissue Res*, 1985, **241**, 639–649.

21. S. Wolter, M. Schuttpelz, M. Tscherepanow, V. D. L. S, M. Heilemann and M. Sauer, *J Microsc-Oxford*, 2010, **237**, 12-22.
22. S. Wolter, A. Löschberger, T. Holm, S. Aufmkolk, M.-C. Dabauvalle, S. van de Linde and M. Sauer, *Nat Methods*, 2012, **9**, 1040–1041.
23. R. Fiolka, L. Shao, E. H. Rego, M. W. Davidson and M. G. Gustafsson, *Proc Natl Acad Sci U S A*, 2012, **109**, 5311-5315.
24. L. Shao, P. Kner, E. H. Rego and M. G. L. Gustafsson, *Nat Methods*, 2011, **8**, 1044-+.
25. P. Kner, B. B. Chhun, E. R. Griffis, L. Winoto and M. G. L. Gustafsson, *Nat Methods*, 2009, **6**, 339-U336.
26. R. Wombacher, M. Heidbreder, S. van de Linde, M. P. Sheetz, M. Heilemann, V. W. Cornish and M. Sauer, *Nat Methods*, 2010, **7**, 717-719.
27. I. Yahiatene, S. Hennig and T. Huser, *Chemical Physics Letters*, 2013, **587**, 1-6.
28. T. Dertinger, R. Colyer, G. Iyer, S. Weiss and J. Enderlein, *P Natl Acad Sci USA*, 2009, **106**, 22287-22292.
29. T. Holm, T. Klein, A. Löschberger, T. Klamp, G. Wiebusch, S. van de Linde and M. Sauer, *ChemPhysChem*, 2014, **15**, 651–654.

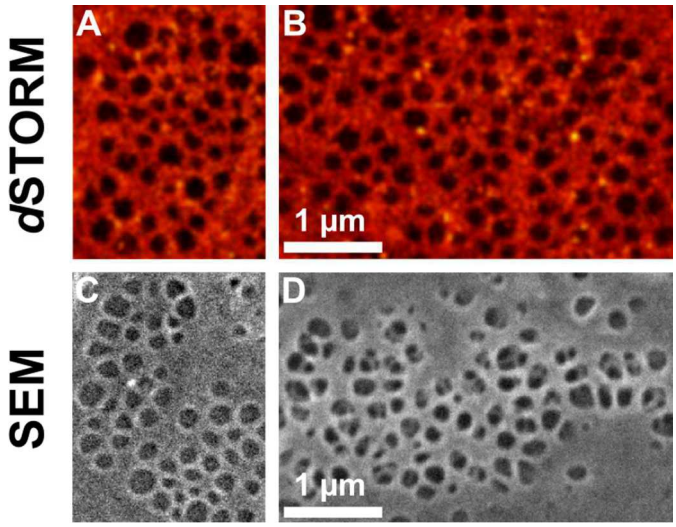

We demonstrate the use of single molecule localization microscopy for resolving structural details of fenestrations in liver sinusoidal endothelial cells.